Ordering process in quenched block copolymers at low temperatures

Y. Yokojima and Y. Shiwa
Division of Materials Science, Kyoto Institute of Technology, Matsugasaki, Sakyo-ku, Kyoto 606-8585, Japan
(Received 20 March 2000)

We have studied domain growth of symmetric diblock copolymers undergoing microphase separation at low temperatures. We introduce a phenomenological nonlinear diffusion model with order-parameter-dependent mobility. Performing two-dimensional simulations, we find that the time-dependent scattering function exhibits dynamical scaling with a logarithmic growth law in the strong segregation limit where surface diffusion is the relevant mechanism for coarsening.

PACS number(s): 64.60.Cn, 61.41.+e, 64.75.+g

I. INTRODUCTION

A linear *A*-*B* diblock copolymer consists of a long sequence of type *A* monomers covalently bonded to a chain of type *B* monomers. A characteristic feature of diblock copolymers is the connectivity between chemically distinct blocks. Because of this severe constraint a phase separation that occurs when the temperature is lowered cannot proceed to a macroscopic scale; unlike binary mixtures of low molecular weight fluids, separation on the microscopic length scale ensues, commonly referred to as microphase separation. In this paper we consider only symmetric *A*-*B* diblock copolymers with equal-length subchains, in which competing interactions between short- and long-range forces result in a stable layered (lamellar) phase with alternating *A*- and *B*-rich domains.

We study the dynamical evolution of the microphase separation after a sudden change of temperature from the disordered state to the state below the coexistence curve. After the quench the system becomes unstable and lamellae of arbitrary orientation emerge. The subsequent evolution of the pattern involves reorientation of lamellae trying to attain parallel stripes of sizable extent. Owing to the existence of a spatial period $(2\pi/k_0)$ of the ordered structure, the dynamics of domain coarsening of the lamellar patterns is quite intriguing in comparison with the case of macroscopic phase separation for which $k_0=0$. It has thus been under extensive investigation (mostly by numerical simulations) [1–4]. Unfortunately, however, no successful theoretical formulation is yet available for the problem, particularly for the asymptotic behavior. Furthermore, many of the previous studies involved a system subjected to a shallow quench or in a weak segregation region.

In contrast to the often investigated weak segregation limit, much less is known about the strong segregation limit or deep quench. By ''deep quench'' we mean quenching to the low temperature region where the equilibrium value of the order parameter is close to that of zero temperature. A deep quench then results in enhanced segregation in that *A*-rich domains are purer in *A* than in the case of a shallow quench. Therefore, if one assumes that the phase separation proceeds by exchange of neighboring *A* and *B* monomers, the probability of such an exchange in the bulk is greatly reduced for deep quenches. Diffusion along the interfaces of domains (to be called surface diffusion) is then expected to play a dominant role.

For spinodal decomposition for which $k_0=0$, the late stage coarsening of domains is characterized by a power-law increase of the typical domain size $\ell \sim t^{\alpha}$ with the growth exponent α, where t is time [5]. The surface-diffusion mechanism for domain growth is known to yield $\alpha=1/4$, in contrast to the usual bulk-diffusion [evaporation-condensation or Lifshitz-Slyozov (LS)] mechanism which gives rise to the LS value $\alpha=1/3$.

For microphase separation, instead, the dynamics becomes exceedingly slow and the usual coarsening mechanism of evaporation-condensation seems to give $\alpha \approx 1/5$ [4]. Because of this much smaller growth exponent, one may naturally wonder whether the power-law growth is followed in deep quenches. This is a highly nontrivial question since suppression of the bulk diffusion would now produce an apparent pinning of the phase separation. It is not even clear that scaling behavior need exist at all in this case. Our result in this paper provides some interesting insights into this problem.

We first introduce a modified time-dependent Ginzburg-Landau-type model for phase-separation dynamics in which the mobility is order-parameter dependent (Sec. II). In Sec. III, we present numerical results obtained from our model. In Sec. IV, interpretation of the result for the strong segregation limit is given. Section V ends this paper with a summary and discussion.

II. DYNAMICAL MODEL

We consider diblock copolymers consisting of *A* and *B* blocks. Each monomer block has a local volume fraction $\phi_i (i=A,B)$. Taking $\phi=\phi_A-\phi_B$ as the order parameter, we assume that the model free energy functional $F\{\phi\}$ consists of short-range and long-range parts:

$$\beta F\{\phi\}=F_s\{\phi\}+F_l\{\phi\}, \tag{1}$$

where $\beta=1/k_BT$, k_B is Boltzmann constant, and T is the temperature. The short-range part is of the usual Ginzburg-Landau form and is given by

$$F_s\{\phi\}=\int d\mathbf{r}\left(\frac{c}{2}(\nabla\phi)^2+W(\phi)\right), \tag{2}$$

where c is a positive constant, $W(\phi)$ is an even function of ϕ with two minima at $\phi=\pm\phi_e$, and $W(\phi)\to\infty$ for $\phi\to\pm\phi_0 (0<\phi_e<\phi_0)$. The long-range part is given by [6]

$$F_l\{\phi\}=\frac{b}{2}\int d\mathbf{r}\int d\mathbf{r}'\,\phi(\mathbf{r})G(\mathbf{r},\mathbf{r}')\phi(\mathbf{r}'), \tag{3}$$

where b is a positive constant, and $G(\mathbf{r},\mathbf{r}')$ is defined through the relation

$$\nabla^2 G(\mathbf{r},\mathbf{r}')=-\delta(\mathbf{r}-\mathbf{r}'). \tag{4}$$

The Coulomb-type repulsive interaction represents the osmotic incompressibility arising from the connectivity of different monomer blocks in each chain, and is inherent in the microphase separation.

With this free energy, we consider the following dynamical model for the time evolution of the order-parameter field:

$$\frac{\partial\phi(\mathbf{r},t)}{\partial t}=\nabla\cdot M(\phi)\nabla\frac{\delta F\{\phi\}}{\delta\phi(\mathbf{r},t)}, \tag{5}$$

where $M(\phi)$ is the diffusion coefficient (mobility). With a constant mobility, the model (5) is the ordinary time-dependent Ginzburg-Landau (TDGL) equation [1]. It has been much used [2–4] in the study of microphase separation in which the domain growth is governed by bulk diffusion. However, as has been noted by several authors [7,8], in the context of macrophase separation kinetics, the mobility should be taken to be dependent on the order-parameter field in order to capture the main features of the constrained cooperative dynamics at low temperatures. For sufficiently low temperatures, where the equilibrium value ϕ_e is close to ϕ_0, the mobility becomes vanishingly small except near the interface between domains; then diffusion occurs only along the interface. We therefore take the mobility in the model (5) to be given by [7,8]

$$M(\phi)=M_0(\phi_0^2-\phi^2), \tag{6}$$

where M_0 is a positive constant. The form (6) takes into account the decrease in bulk diffusion as the temperature is lowered, and contains the surface-diffusion effect automatically. It is convenient in the following to use the scaled order parameter $\psi\equiv\phi/\phi_e$. Setting $M_0\phi_0^2=1$ without loss of generality, Eq. (6) can be written as

$$M(\psi)=1-a^2\psi^2. \tag{7}$$

Here $a\equiv\phi_e/\phi_0$ measures the depth of the quench, the value of which varies from 0 to 1 as temperature is reduced, and $a=1$ at $T=0$ in particular.

We have carried out computer simulations of the above model. Simulations have been done by means of the cell-dynamical-system (CDS) method [9]. At each time step t we assign a scalar variable $\psi(n,t)$ corresponding to the order parameter field $\psi(\mathbf{r},t)$ to each lattice site (nth cell) on 256 $\times$256 square cells with periodic boundary conditions. The Laplacian is replaced by the isotropically discretized equivalent $[\nabla^2]_d$, involving both nearest and next-nearest neighbors:

$$[\nabla^2]_d X=6(\langle\langle X\rangle\rangle-X), \tag{8}$$

where $\langle\langle X\rangle\rangle=(1/6)\Sigma_{nn}X+(1/12)\Sigma_{nnn}X$, $nn(nnn)$ representing nearest (next-nearest) neighbor cells. The form of the force $dW/d\psi$ is taken to be

$$-\frac{dW(\psi)}{d\psi}=A\tanh(\tilde{A}\psi)-\psi, \tag{9}$$

where $\tilde{A}=\operatorname{arctanh}(1/A)$, so that the minima of $W(\psi)$ are at $\psi=\pm1$ for any $A>0$, as required.

The local conservation law is implemented by considering the Kawasaki exchange dynamics [8]. Thus we obtain the CDS equation corresponding to Eq. (5), which reads

$$\psi(n,t+1)=\psi(n,t)+\langle\langle\mathcal{C}(n,j;\operatorname{sgn}[\mathcal{J}(n,t)-\mathcal{J}(j,t)])\times[\mathcal{J}(n,t)-\mathcal{J}(j,t)]\rangle\rangle, \tag{10}$$

with

$$\mathcal{C}(i,j;\alpha)=[1+\alpha a\psi(j,t)][1-\alpha a\psi(i,t)] \tag{11}$$

and

$$\mathcal{J}(n,t)=A\tanh[\tilde{A}\psi(n,t)]-\psi(n,t)+D[\langle\langle\psi(n,t)\rangle\rangle-\psi(n,t)]+B[\nabla^{-2}]_d\psi(n,t). \tag{12}$$

D and B are positive constants corresponding to c and b in Eqs. (2) and (3), respectively. The operator $[\nabla^{-2}]_d$ is the inverse of the CDS Laplacian $[\nabla^2]_d$, and is computed using a standard fast-Fourier-transform technique.

In passing, reference may here be made to a linearized analysis of Eq. (10). The wave number k_e of the equilibrium pattern is obtained as the solution of $2J_0(k_e)+J_0(\sqrt{2}k_e)=3(1-\sqrt{B/6D})$, where $J_0(z)$ is the Bessel function of the first kind. One also finds that the interface thickness ξ can be estimated from the equation $2J_0(k_d)+J_0(\sqrt{2}k_d)=3[1+(1-A\tilde{A})/D]$ to be $\xi=2\pi/k_d$.

III. NUMERICAL RESULTS

We have performed a numerical simulation of Eqs. (10)–(12) with the initial condition for the ψ's consisting of uniformly distributed random values between ±0.05. Each run is repeated with five different initial configurations to average over. We set the constant a at either 0 or 1, and call these cases the weak segregation limit and the strong segregation limit, respectively. Figure 1 exhibits the patterns obtained after 10^5 time steps for these limits with the same initial condition.

We computed the circularly averaged scattering function $S(k,t)$. It is defined by $S(k,t)=\langle\psi(\mathbf{k},t)\psi(\mathbf{k},t)\rangle$ where the angular brackets refer to an ensemble average as well as an average over the orientation of the wave vector $\mathbf{k}$; $\psi(\mathbf{k},t)$ is the Fourier transform of the order parameter, $\psi(\mathbf{k},t)=\Sigma_{\mathbf{r}}e^{i\mathbf{k}\cdot\mathbf{r}}\psi(\mathbf{r},t)$, and $\mathbf{k}$ can take values $\mathbf{k}=(2\pi/L)(m_x,m_y)$ where m_x and m_y have integer values between $-L/2$ and $L/2-1$ for a lattice of size $L\times L$ ($L=256$). The order-parameter profiles are hardened before computing the scattering function using the transformation $\psi\to\operatorname{sgn}\psi$. We fitted $S(k,t)$ to a squared Lorentzian form,

$$S(k,t)=a^2/[(k^2-b^2)^2+c^2]^2, \tag{13}$$

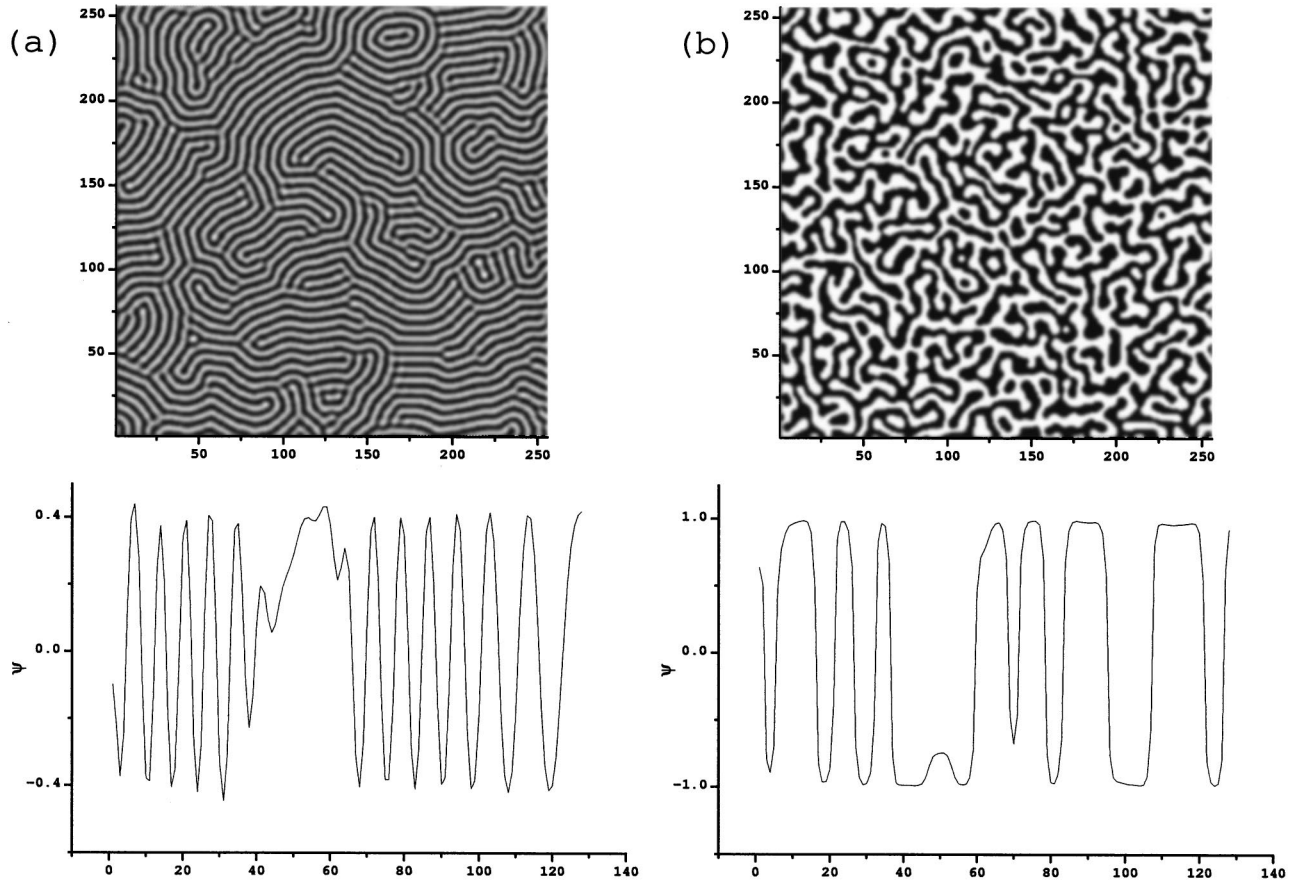

FIG. 1. The ψ field after 10^5 time steps for $a=0$ (a) and 1.0 (b) with the same initial condition. The bright regions denote positive values of ψ, while the dark ones are for negative ψ. The lower part exhibits the cross section along the horizontal line in the middle portion of the pattern above, and represents the domain-wall structure. The numbers along the vertical axes denote order-parameter values.

where the fitting parameters a,b, and c should not be confused with the basic constants of our model. We have thus extracted the full width at half maximum $\Delta k(t)$ and the peak height $S_M(t)$ of $S(k,t)$. (We have also performed a fit to a Gaussian form and this made no difference to our results.) As an example, the time evolution of $S(k,t)$ for the strong segregation limit is shown in Fig. 2(a), and the solid curve in Fig. 2(b) is the best fit to the data using the form (13).

Before we proceed, a remark is in order. As far as the growth exponent is concerned, systems of sizes 256^2 and 512^2 show almost identical results in the case of the weak segregation limit (see Ref. [4]). For the strong segregation limit, the correlation range is much smaller than $L/2$ [see Fig. 4(b) below]. Therefore we judge that finite-size effects were avoided in our numerical simulations.

A. Weak segregation limit ($a=0$)

The parameters used for this case are $A=3.7$, $B=0.02$, and $D=0.036$, so that $k_e=1.00$ and $\xi=3.8$. Since the equilibrium lamellar spacing (periodicity) λ may be estimated by the relation $\lambda=2\pi/k_e$, the chosen set of parameters yields $\xi/\lambda=0.60$, corresponding in fact to weakly segregated lamellae. Figure 3(a) shows the time dependence of the peak position $k_p(t)$ of $S(k,t)$. Notice that at late times the system has almost attained the equilibrium lamellar thickness, which could not be distinguished from the value of $2\pi/k_e$ determined from the linear analysis.

Even in that time region, however, narrowing of the scattering profile and an increase of peak intensity occurred gradually, indicating domain coarsening processes. In Fig. 3(b) we plot the width $\Delta k(t)$ and peak height $S_M(t)$ as a function of time. Identifying $2\pi/\Delta k(t)$ with the average domain size $\ell(t)$, we find that this characteristic length scale is well fitted by a power law $\ell(t)\propto t^{\alpha}$ with $\alpha\approx 1/5$. The same scaling is found for the peak height, $S_M(t)\sim t^{\beta}$ with $\beta=\alpha$. This implies that the scattering function obeys the scaling law $S(k,t)=\ell(t)f((k-k_e)\ell(t))$, f being a scaling function. All these results just confirm the previous findings of numerical work [4] done in the weakly segregated regime.

Before proceeding to the strong segregation case, a couple of comments are in order. In contrast to the strong segregation limit where bulk diffusion is essentially inhibited, surface diffusion is expected to be an irrelevant effect in the weak segregation kinetics. We have performed simulations with the same values of parameters except for the a value. As expected, for $a\neq 0$ the numerical data for $\Delta k(t)$, $k_p(t)$, and $S_M(t)$ revealed little change from the results given for $a=0$ in Fig. 3.

The power-law growth with exponent $\approx 1/5$ has also been found in the pattern dynamics of Rayleigh-Bénard convective rolls [10]. It is thus suggested [4] that these stripe-pattern forming systems (i.e., block copolymers and thermal convective systems) belong to the same universality class of coarsening dynamics. However, we have no good theoretical

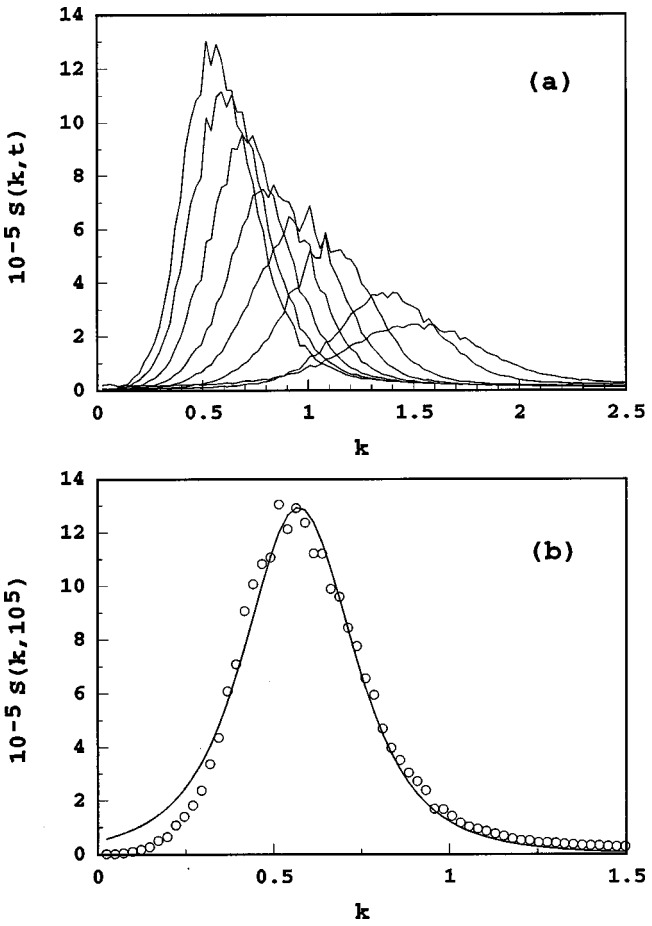

FIG. 2. (a) Time evolution of the circularly averaged scattering function $S(k,t)$ for the strong segregation limit; $S(k,t)$ is in arbitrary units, and the times are, from lowest to highest, 400,1000,4000,8000,15 000,30 000,60 000, and 100 000. (b) $S(k,t)$ after 10^5 time steps as a function of the wave number. The solid curve is the best fit to the data (open circles) using a squared Lorentzian form.

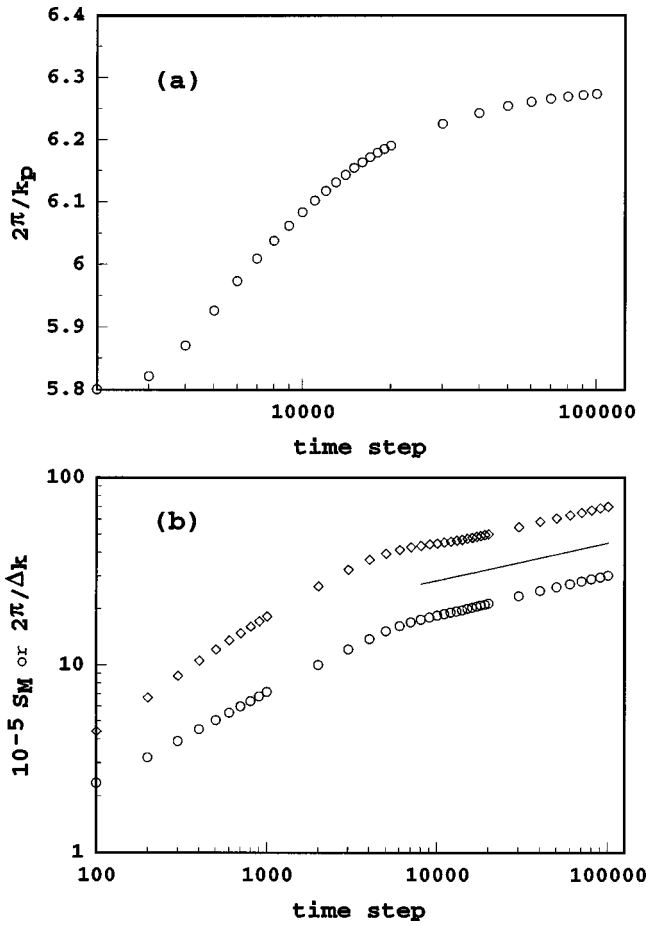

FIG. 3. (a)A lin-log plot of the peak position k_p vs t, and (b) a log-log plot of the width Δk ($\diamond$) and the peak intensity S_M ($\bigcirc$) vs t of the scattering function for the weak segregation limit. The inserted line has the slope 0.20.

understanding of the observed growth exponent at present.

B. Strong segregation limit ($a=1$)

The parameter values we now use are $A=3.7, B=0.0001$, and $D=0.02$, so that $\xi/\lambda=0.10$. In Fig. 2(a) we show a plot of $S(k,t)$ versus t. We observe that even at $t=10^5$ the peak position is still moving toward the equilibrium position, which should be close to $k_e=0.30$. See Fig. 3(a) for comparison. The peak height and the length scale data obtained from the fitting are displayed in Fig. 4 as a function of time. Notice that the data are plotted on a semilogarithmic scale. At late times we get a good straight-line fit to the data in Fig. 4, demonstrating the scaling $S_M(t)\sim 2\pi/\Delta k(t)\sim 2\pi/k_p(t)\sim \log_{10}t$. In particular, writing $2\pi/\Delta k(t)=\nu\log_{10}(t/t_0)+\text{const}$ and $2\pi/k_p(t)=\tilde{\nu}\log_{10}(t/t_1)+\text{const}$, we find $\nu=\tilde{\nu}\approx 3.7\pm 0.4$. This suggests the existence of a characteristic length scale with a logarithmic growth law. [Note that the value of the slope of the $S_M(t)$ vs $\log_{10}t$ curve need not equal the above ν value. This is because the ''exponent'' γ of the growth law $\gamma\log_{10}t(=\log_{10}t^{\gamma})$ contains a normalization constant that one chooses for the corresponding quantity.] In the next section, interpretation of the logarithmic behavior in terms of interacting kinks is given.

IV. KINK DYNAMICS INTERPRETATION

In the strong segregation limit at $T=0$, the flux is localized at the interface, and only the tangential (to the interface) component gives a dominant contribution on the right-hand side of the evolution equation (5). In order to study this surface (interfacial) diffusion effect on domain growth, we resort to a phase dynamics description [11,12]. The basic assumption here is that at late stages of coarsening the surface-diffusion mechanism is associated with a slow variation of the wave vector along the interface of lamellar patterns. This then allows us to expect that the interfacial diffusion behavior of our interest is present already in the phase-field description of the constant-diffusion model.

We thus begin with the dynamic equation.

$$\frac{\partial\phi}{\partial t}=\nabla^2[-(\tau+\nabla^2+b\nabla^{-2})\phi+\phi^3], \tag{14}$$

where the form of the potential $W(\phi)$ in Eq. (2) has been chosen to be the usual one: $W(\phi)=(\tau/2)\phi^2+(1/4)\phi^4$, τ

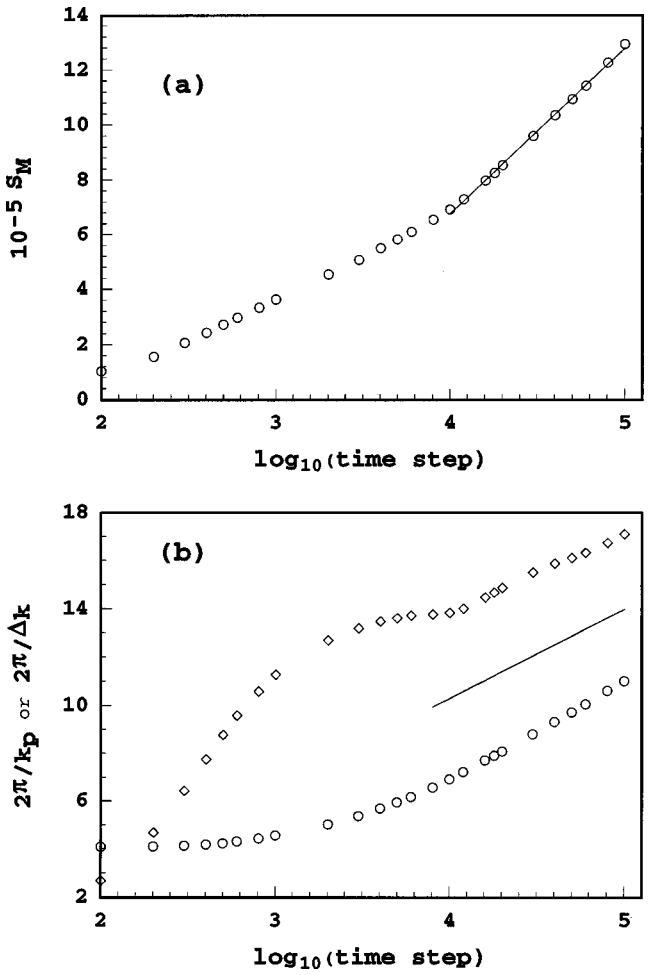

FIG. 4. A lin-log plot of (a) the peak height S_M vs t, and (b) the width Δk ($\diamond$) and the peak position k_p ($\bigcirc$) vs t of the scattering function for the strong segregation limit. The straight line inserted in (b) has the slope 3.7, while in (a) it has the slope 6.0.

being a constant. We seek slowly varying lamellar solutions to Eq. (14). To that end we introduce slow space and time variables

$$X=\delta x, \quad Y=\delta y, \quad T=\delta^2 t \tag{15}$$

and a slow phase variable

$$\Theta(X,Y,T)=\delta\theta(x,y,t). \tag{16}$$

The dimensionless parameter δ is the ratio of lamellar size to system size, and is an expansion parameter of our subsequent analysis. The local wave vector of lamellae is given by

$$\mathbf{k}(X,Y,T)=\nabla\theta=\nabla_{\mathbf{X}}\Theta \tag{17}$$

with $\mathbf{X}=(X,Y)$. We develop the solution as an expansion in δ:

$$\phi(x,y,t)=\sum_{n=0}\delta^n\phi^{(n)}(\theta;X,Y,T), \tag{18}$$

where each $\phi^{(n)}$ is 2π periodic in θ. The phase equation for $k(\Theta)$ arises as a solvability condition for $\phi^{(1)}$. Referring the reader to Ref. [13] for details, we thus obtain

$$\omega^{-1}(k)\partial_T\Theta=D_{\parallel}(k)(\hat{\mathbf{k}}\cdot\nabla)k+D_{\perp}(k)k\nabla\cdot\hat{\mathbf{k}}+\delta^2\mathcal{R}\nabla^4\Theta \tag{19}$$

where $\hat{\mathbf{k}}=\mathbf{k}/k$. The explicit forms for $\omega(k)$, $D_{\parallel}(k)$, and $D_{\perp}(k)$ are given in Ref. [13]. In Eq. (19) we have added a regularization term ($\propto\delta^2$) corresponding to the bending of the phase surface so that Eq. (19) may describe all features of patterns in both the smooth regions and the regions with line and point defects [12]. The coefficient $\mathcal{R}$ will be determined later.

Let us now examine a special class of solution of the phase diffusion equation (19) when k approaches the wave number of equilibrium lamellae [which turns out to be very close to $k_e\equiv b^{1/4}$, the value determined from Eq. (14) by linear analysis] and the far field is almost a field of straight parallel lamellae. Because k_e is also the wave number for the onset of the zigzag instability [13], the resistance of the lamellae to perturbations with variations along their axes weakens when $k\to k_e$. If $k=k_e+O(\delta)$, in accordance with our slow scales (15), the wave number along the lamellae is of order $\sqrt{\delta}$. Thus we put [12]

$$\Theta(X,Y,T)=k_eX+\delta\Psi(\xi\equiv X/k_e,\eta\equiv Y/\sqrt{\delta},T), \tag{20}$$

and find

$$\omega^{-1}\Psi_T=(D_{\parallel}/k_e^2)[\Psi_{\xi\xi}+2\Psi_{\eta}\Psi_{\xi\eta}+(\Psi_{\eta})^2\Psi_{\eta\eta}] +(D_{\perp}/\delta)\Psi_{\eta\eta}-\mathcal{R}\Psi_{\eta\eta\eta\eta}, \tag{21}$$

to the lowest order in δ. Here in Eq. (21) $\omega^{-1}\equiv\omega^{-1}(k_e), D_{\parallel}\equiv D_{\parallel}(k_e), D_{\perp}\equiv D_{\perp}(k\to k_e)$, and we have used the fact that $\omega^{-1}=O(1), D_{\parallel}=O(1)$, and $D_{\perp}=O(\delta)$. More explicitly,

$$\omega^{-1}=\frac{2}{3}k_e^2\epsilon, \quad D_{\parallel}=\frac{8}{3}k_e^4\epsilon,$$

$$D_{\perp}=\frac{4}{3}k_e^2\epsilon[2\Psi_{\xi}+(\Psi_{\eta})^2]\delta, \tag{22}$$

where $\epsilon\equiv(\tau-\tau_c)/k_e^2$ measures the distance from threshold $\tau_c\equiv 2k_e^2$ for a lamella-forming instability. Therefore we obtain

$$\Psi_T=4\Psi_{\xi\xi}+8\Psi_{\eta}\Psi_{\xi\eta}+6(\Psi_{\eta})^2\Psi_{\eta\eta}+4\Psi_{\xi}\Psi_{\eta\eta}-\tilde{\mathcal{R}}\Psi_{\eta\eta\eta\eta} \tag{23}$$

with $\tilde{\mathcal{R}}\equiv 3\mathcal{R}/2k_e^2\epsilon$. The easiest way to find the coefficient $\mathcal{R}(\tilde{\mathcal{R}})$ is to match Eq. (23) to the corresponding phase equation in the small amplitude limit [11,12]. The latter equation can be obtained from the envelope (amplitude) equation for the model (14), which reads [13]

$$\frac{\partial A}{\partial T}=\left[k_e^4-3k_e^2|A|^2+4k_e^2\left(\frac{\partial}{\partial X}-\frac{i}{2k_e}\frac{\partial^2}{\partial Y^2}\right)^2\right]A, \tag{24}$$

where

$$\phi(x,y,t)=\epsilon^{1/2}A(X,Y,T)e^{ik_ex}+c.c. \tag{25}$$

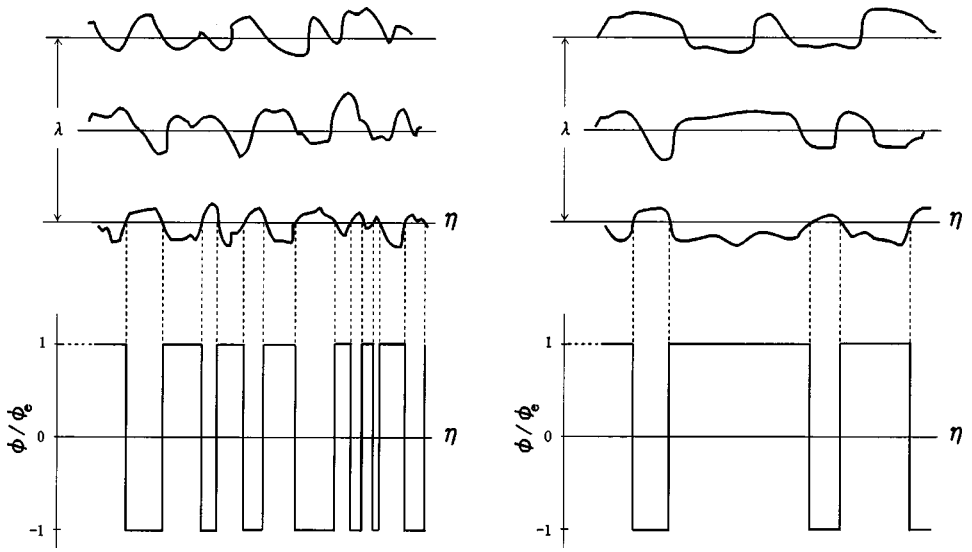

FIG. 5. A schematic representation of the local lamellar configurations (in two dimensions) at two different times in the strong segregation limit. Top: The curves indicate domain walls (interfaces), λ being the spatial period of the lamellae. Bottom: A cross section along the lowest η axis. The kink configuration at a much later time after kink-antikink annihilation is shown on the right.

with $X=\epsilon^{1/2}x$, $Y=\epsilon^{1/4}y$, and $T=\epsilon t$. Setting $A(X,Y,T)=A_0\exp[i\Psi(X,Y,T)]$ in Eq. (24), and taking the imaginary part of the resulting equation, we reproduce exactly Eq. (23) with $\tilde{\mathcal{R}}=1$.

In the strong segregation regime where the dominant driving force of coarsening is surface diffusion, Ψ varies faster along the lamellae than across them. Hence in Eq. (23) we may put $\Psi_\xi \approx$ const. Denoting this constant as κ (which represents the distance from k_e), we then obtain

$$\Psi_T \simeq 6(\Psi_\eta)^2\Psi_{\eta\eta}+4\kappa\Psi_{\eta\eta}-\Psi_{\eta\eta\eta\eta}. \tag{26}$$

Equivalently, with $\Phi\equiv\Psi_\eta$, we have

$$\partial_T\Phi=2\partial_\eta^2\Phi^3+4\kappa\partial_\eta^2\Phi-\partial_\eta^4\Phi=\partial_\eta^2\frac{\delta\hat{F}}{\delta\Phi},$$

$$\hat{F}=\int d\eta[2\kappa\Phi^2+\tfrac{1}{2}\Phi^4+\tfrac{1}{2}(\partial_\eta\Phi)^2]. \tag{27}$$

This is the one-dimensional TDGL equation for the conserved field. Note that $\kappa>0$ in the late stages of coarsening as can be seen from Fig. 2. Hence we expect that $\Phi\to 0$ as $t\to\infty$. This suggests the following picture for the evolution of the order parameter ϕ. Since in the late stage of microphase separation in which we may restrict ourselves to the wave number region where $k\sim k_e$, ∇^2 in Eq. (14) may be replaced [14] by $-k_e^2$. Note also that, due to the absence of spatial periodicity in $\Phi(\eta)$, the order parameter ϕ also cannot have periodicity along η axis. Hence the evolution of ϕ is expected to be governed by the so-called (one-dimensional) model-*A* dynamics [15]. Recall that we are concerned with the late stages of phase ordering in the strong segregation limit. Thus the domain-wall profiles are those of kinks, and the domain coarsening proceeds via annihilation of kink-antikink pairs along the interface. Figure 5 illustrates this scenario schematically.

For model *A*, the annihilation processes of interacting kinks have been studied by Kawasaki *et al.* [16–18]. The attractive interaction between an adjacent kink and antikink decays exponentially with their separation distance, and the time required to eliminate the pair is also exponentially large. This results in a logarithmic growth law, namely, the domain size $\ell(t)$ evolves according to

$$\ell(t)=\nu\xi\ln(t/t_0) \tag{28}$$

with some constants ν and t_0. The ξ in Eq. (28) is the effective width of the domain wall.

Let us compare our result from computer simulations with the above Eq. (28). For the parameters used in our CDS simulation of the strong segregation limit, we estimate $\xi=2.2$. Identifying the characteristic width $\Delta k(t)$ [or the peak position $k_p(t)$] of the scattering function $S(k,t)$ with $2\pi/\ell(t)$, we find $\nu=1.0\pm 0.1$. This value is to be compared with the result of Nagai and Kawasaki [17]; they performed a molecular dynamics simulation of the one-dimensional kink equation deduced from the model *A*, and reported the relation (28) with $\nu=3.5\pm 0.2$. The smallness of the ν value that we have extracted from our data in comparison with the Nagai-Kawasaki result for the one-dimensional kink system should be ascribed to the higher dimensionality of our system.

As mentioned already, the pairwise attractive force between kinks is exponentially weak. A very small influence (either external or due to defects) can then act to pin the patterns. It gives rise to a glassy dynamics analogous to the slow dynamics of spin glasses or ordinary glasses. [In this connection we remark that in the glass literature [19] it has been suggested that the average domain length (or the so-called dynamical correlation length) $\xi_g(t)$ after a quench to a very low temperature T grows as $\xi_g(t)\sim t^{BT}$ with a constant *B*.] In two dimensions defects other than kinks are self-generated dynamically. Therefore the theoretical description of our ordering process should be two dimensional, although it can be reduced approximately to the one-dimensional problem as we showed above. This also explains why we observe labyrinthine patterns such as those in Fig. 1(b), whose typical size is of the order of just a few lamellae spacings [cf. Fig. 4(b)].

V. SUMMARY AND DISCUSSION

We have studied the effect of bulk and surface diffusion on the domain coarsening of microphase separation in

diblock copolymers. We expect our TDGL model to be in the same dynamical universality class as a suitable model with order-parameter-dependent mobility for the Rayleigh-Bénard convection system. Although the order parameter for block copolymer lamellar phases is a conserved variable, nonconserved dynamics are appropriate in the late stages of coarsening because of our restriction to $k \approx k_0$, the wave number of the final equilibrium pattern. In the case of a constant diffusion coefficient this is in fact borne out by numerical work [4].

The strong segregation limit ($a=1$) studied in the present paper is interesting only insofar as it is experimentally relevant, since the effective quench depth a is not unity at any finite temperature. However, as stressed by Ohta [20], the value of the parameter a can be very close to unity even at the temperature $T=T_c/2$ where T_c is the critical temperature; for example, according to Onsager's exact solution of the two-dimensional Ising model, $a=0.999$ for $T/T_c=0.5$. Therefore the description presented in Sec. III B should also be valid at finite and low temperatures.

As far as a system undergoing spinodal decomposition is concerned, both analytical [20] and numerical [21] studies have shown that the algebraic behavior of domain growth at low temperatures changes continuously with time from a 1/4 to a 1/3 power law; as the growing domains become sufficiently coarsened, the bulk-diffusion mechanism takes over eventually. An estimation has been given [20] of the critical domain size (ℓ_c) for which the crossover occurs. It is estimated as

$$\ell_c \sim \frac{\xi}{1/a^2-1}, \tag{29}$$

and in the region $\ell < \ell_c$ surface diffusion is dominant while for $\ell > \ell_c$ bulk diffusion governs the coarsening.

We note that the order estimate (29) is derived on the basis of the interface equation of motion. When applied to a microphase-separating system [3], the interface-equation approach simply fails to reproduce the growth exponent $\alpha \approx 1/5$. However, having no successful theory at hand, we will be content to use the expression (29) in characterizing the putative crossover of our copolymer systems in the strong segregation regime. We then estimate that for parameter values used in Sec. III B the crossover from $\ln t$ to $t^{1/5}$ growth occurs at $t \sim 10^{350}$ time steps for $T=T_c/2$. Therefore logarithmic growth seems to be experimentally relevant at low temperatures, holding over an appreciable time interval [22].

In order to probe the expected crossover to power-law growth, we have performed simulations with variable values of a with $\xi/\lambda = 0.10$. However, no evidence of a crossover was observed. For example, at values of a and ξ for which most of the time range is predicted by Eq. (29) to be bulk-diffusion dominated, the data were not well fitted by a power-law scaling such as we have found for the weak segregation regime. From this result combined with those presented in Sec. III, we conclude that (i) in the weak segregation regime [$\xi/\lambda \sim O(1)$], power-law scaling $\ell(t) \sim t^{\alpha}$ with $\alpha \simeq 1/5$ is obeyed; (ii) in the strong segregation regime [$\xi/\lambda \ll 1$], no scaling law is at work except at low temperatures ($a \approx 1$) for which logarithmic growth characterizes the late-stage ordering kinetics. This indicates the relevance of the parameter ξ/λ, which is absent in spinodal decomposition, for the ordering process in quenched block copolymers. However, we do not have a general answer to the question of how the measurable quantities such as $\ell(t)$ are related to ξ/λ. Obviously a theoretical understanding of the $t^{1/5}$ growth is a crucial prerequisite, but so far this has not been reached even on a qualitative level.

We have found that for the strong segregation limit of deep quenches the late evolution becomes exceedingly slow and the system remains in a quasipinned state. This is due to the existence of a nonequilibrium partially ordered state that becomes stable over an appreciable time interval in the presence of topological defects such as disclinations and phase grain boundaries. The absence of those defects in the one-dimensional (1D) kink system makes less reliable the extrapolation of the result for the 1D kink model to the description of higher dimensional systems. We hope our results in this paper motivate further theoretical and experimental work toward understanding the role of various defects in the coarsening process of stripe patterns.

ACKNOWLEDGMENTS

Y.S. is grateful to T. Nagai and T. Kawakatsu for informative conversations on kink dynamics. We also thank T. Kawakatsu for sending copies of related papers.

[1] Y. Oono and Y. Shiwa, Mod. Phys. Lett. B **1**, 49 (1987).
[2] Y. Oono and M. Bahiana, Phys. Rev. Lett. **61**, 1109 (1988); F. Liu and N. Goldenfeld, Phys. Rev. A **39**, 4805 (1989); A. Chakrabarti, R. Toral, and J.D. Gunton, Phys. Rev. Lett. **63**, 2661 (1989); A. Chakrabarti, R. Toral, and J.D. Gunton, Phys. Rev. A **44**, 6503 (1991); A. Chakrabarti and J.D. Gunton, Phys. Rev. E **47**, R792 (1993).
[3] M. Bahiana and Y. Oono, Phys. Rev. A **41**, 6763 (1990).
[4] Y. Shiwa, T. Taneike, and Y. Yokojima, Phys. Rev. Lett. **77**, 4378 (1996); J.J. Christensen and A.J. Bray, Phys. Rev. E **58**, 5364 (1998).
[5] For a recent review, see A.J. Bray, Adv. Phys. **43**, 357 (1994).
[6] L. Leibler, Macromolecules **13**, 1602 (1980); T. Ohta and K. Kawasaki, *ibid.* **19**, 2621 (1986).
[7] J.W. Cahn, C.M. Elliot, and A. Novick-Cohen, Eur. J. Appl. Math. **7**, 287 (1996), and references therein; J.S. Langer, N. Bar-On, and H.D. Miller, Phys. Rev. A **11**, 1417 (1975); K. Kitahara and M. Imada, Suppl. Prog. Theor. Phys. **64**, 65 (1978); T. Ohta, J. Phys. C **21**, L361 (1988).
[8] K. Kitahara, Y. Oono, and D. Jasnow, Mod. Phys. Lett. B **2**, 765 (1988).
[9] Y. Oono and S. Puri, Phys. Rev. Lett. **58**, 836 (1987); Phys. Rev. A **38**, 434 (1988); S. Puri and Y. Oono, *ibid.* **38**, 1542 (1988).
[10] K.R. Elder, J. Viñals, and M. Grant, Phys. Rev. Lett. **68**, 3024 (1992); Phys. Rev. A **46**, 7618 (1992); M.C. Cross and D.I.

Meiron, Phys. Rev. Lett. **75**, 2152 (1995); Q. Hou, S. Sasa, and N. Goldenfeld, Physica A **239**, 219 (1997).
[11] M.C. Cross and A.C. Newell, Physica D **10**, 299 (1984).
[12] T. Passot and A.C. Newell, Physica D **74**, 301 (1994).
[13] Y. Shiwa, Phys. Lett. A **228**, 279 (1997).
[14] G.H. Fredrickson and K. Binder, J. Chem. Phys. **91**, 7265 (1989); G.H. Fredrickson, J. Rheol. **38**, 1045 (1994).
[15] P.C. Hohenberg and B.I. Halperin, Rev. Mod. Phys. **49**, 435 (1977).
[16] K. Kawasaki and T. Ohta, Physica A **116**, 573 (1982).
[17] T. Nagai and K. Kawasaki, Physica A **120**, 587 (1983).
[18] K. Kawasaki and T. Nagai, Physica A **121**, 175 (1983); T. Nagai and K. Kawasaki, *ibid.* **134**, 483 (1986); K. Kawasaki, A. Ogawa and T. Nagai, Physica B&C **149**, 97 (1988); see also F. de Pasquale, P. Tartaglia, and P. Tombesi, Phys. Rev. A **31**, 2447 (1985); A.D. Rutenberg and A.J. Bray, Phys. Rev. E **50**, 1900 (1994).
[19] P. Sollich and M.R. Evans, Phys. Rev. Lett. **83**, 3238 (1999); E. Marinari, G. Parisi, F. Ricci-Tersenghi, and J.J. Ruiz-Lorenzo, e-print cond-mat/9910232.
[20] T. Ohta, J. Phys. C **21**, L361 (1988).
[21] A.M. Lacasta, A. Hernández-Machado, and J.M. Sancho, Phys. Rev. B **45**, 5276 (1992); S. Puri, A.J. Bray, and J.L. Lebowitz, Phys. Rev. E **56**, 758 (1997).
[22] Actually, we have found that the logarithmic growth holds on times longer than those shown in Fig. 4, up to $t=2\times10^5$. However, we did not explore the more extended time regime because it is extremely time consuming.